JOURNAL OF Materials CHEMISTRY

Disk-like liquid crystals of transition metal complexes

Part 20.‡—Pursuit of chemistry to directly visualize van der Waals interactions

Kazuchika Ohta,*† Mayumi Ikejima, Mitsuo Moriya, Hiroshi Hasebe and Iwao Yamamoto

Department of Functional Polymer Science, Faculty of Textile Science and Technology, Shinshu University, 386 Ueda, Japan

This work reports on mesomorphic thermochromism caused by metal centres leading to visualization of van der Waals interactions. We succeeded in obtaining columnar liquid crystals exhibiting very interesting thermochromism by introduction of long chains into disk-like bis(glyoximato) d^8 metal(II) complexes. These long-chain-substituted Ni^{II}, Pd^{II} and Pt^{II} complexes, $(C_nO)_8$-M, containing one-dimensional metal chain change color according to the metal–metal stacking distance. With increasing temperature, the metal–metal distance increases leading to an enlargement of the band gap between the filled nd_{z^2} valence band and the empty $(n+1)p_z$ conduction band of the central metal. Generally speaking, when mesomorphic materials are heated, the peripheral alkyl chains melt, whereas the central aromatic part remains rigid. Adjacent peripheral long chains tend to lie within the van der Waals radius at lower temperatures, which results in a shortening of the distance between the central d^8 metals in the present $(C_nO)_8$-M systems. This 'fastener effect' of the van der Waals interaction of peripheral long chains is weakened with increasing temperature, leading to visible color changes due to the nd_{z^2}–$(n+1)p_z$ interaction in the central metal chain. The 'apparent pressures' of the long chains in the $(C_nO)_8$-M complexes have been estimated from the shift coefficient of the d–p band *vs.* pressure for the corresponding non-substituted metal complexes.

1 Introduction

Is it possible to directly visualize van der Waals interactions? It is well known that the main intermolecular force in molecular condensed phases is van der Waals interaction. If a molecular solid is gradually heated, the condensation force by this van der Waals interaction gradually becomes weaker. It is especially interesting that this force weakening causes the phase changes as solid(crystal)→liquid crystal→liquid. These changes are attributable to the molecular structure of liquid crystalline materials. Many liquid crystals are, generally, composed of aromatic groups at the molecular center and long alkyl chains at the surroundings. On gradually heating liquid crystalline materials, the peripheral alkyl chains begin to melt, whereas the central aromatic part remains essentially rigid. This is the reason why liquid crystalline phases appear before completely melting into the liquid phase. In this context, can one directly visualize van der Waals interactions of alkyl chains changing with temperature? This is our starting viewpoint for the present work.

Recently, we investigated a novel phenomenon of 'mesomorphic thermochromism due to metal centres'.[2–4] This phenomenon is largely concerned with an attempt to directly visualize van der Waals interactions. Recently, we succeeded in obtaining discotic columnar liquid crystals exhibiting very interesting thermochromism by introduction of long chains into a disk-like molecule, bis(diphenylglyoximato)M (M = Ni, Pd or Pt). We found that these long-chain-substituted Ni^{II}, Pd^{II} and Pt^{II} complexes having a one-dimensional columnar structure show temperature dependent color changes, *i.e.*, thermochromism. With increasing temperature, the metal–metal distance increase leads to an enlargement of band gap between the filled nd_{z^2} valence band and the empty $(n+1)p_z$ conduction band of the metal. This results in a blue-shift of the electronic transition spectrum which is directly connected with d–p interactions between the upper and lower metals in the one-dimensional metal chains. The present d^8-metal complexes (Fig. 1) were synthesized by introduction of eight long alkoxy groups into core bis(diphenylglyoximato)metal(II) moieties which exhibit piezochromism as reported by Shirotani *et al.*[5–9] They reported that the non-substituted bis(diphenylglyoximato)platinum(II) complex is red–brown under atmospheric pressure but green under 0.69 GPa. Suprisingly, the present alkoxy-chain-substituted bis(diphenylglyoximato)platinum(II) complexes already show a green color even under atmospheric pressure as if 0.69 GPa of external high pressure were applied. This 'apparent pressure' is attributed to an effect of self-pressing by van der Waals interaction of the peripheral chains, *i.e.*, a 'fastener effect'.[10–15] The neighboring peripheral alkyl chains tend lie within the van der Waals radius at lower temperatures, which results in shortening the distance between the central d^8 metals in the one-dimensional columnar structure. The fastener effect of the van der Waals interaction is weakened with increasing temperature, which leads to a color change due to an alteration of the d–p interaction in the metal chain. Hence, this color change can be directly visualized. For example, the present alkoxy-chain-substituted bis(diphenylglyoximato)platinum(II) complexes are green at r.t., and turn red in the mesophase with increasing temperature.

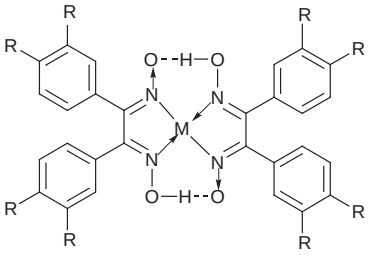

Fig. 1 Structural formula of long chain-substituted bis(diphenylglyoximato)metal(II) complexes

†E-mail: ko52517@giptc.shinshu-u.ac.jp
‡Part 19: ref. 1.

2 Experimental

2.1 Synthesis

The synthetic routes for $(C_nO)_8$-Pt ($n=4$–14) **3** and $(C_{12})_8$-Ni **4** are shown in Scheme 1. Detailed procedures of the preparation of precursors **5** and **6** have described previously.[16] The $(C_nO)_8$-Pt ($n=4$–14) and $(C_{12})_8$-Ni complexes were prepared by the reaction of the corresponding α-diketones, **5** and **6**, with hydroxylamine hydrochloride in the reaction solvent, followed by addition of an ethane-1,2-diol or propane-1,3-diol solution of the metal salt and then neutralization with glacial acetic acid. Detailed procedures are presented only for the representative $(C_{14}O)_8$-Pt complex. Table 1 summarizes reaction solvents, solvents for the metal salt, elemental analysis data, yields, and colors of the complexes.

Bis[1,2-bis(3,4-di-*n*-tetradecyloxyphenyl)ethanedione dioximato]platinum(II) 3, $(C_{14}O)_8$-Pt. To 313 ml ethanol, hydroxylamine hydrochloride (12.9 g, 185 mmol) and 85% potassium hydroxide (12.9 g, 185 mmol) were added and the mixture was stirred vigorously for *ca.* 1 h and filtered to remove precipitates. 3,3′,4,4′-Tetradecyloxybenzil **5** (3.00 g, 2.83 mmol) was added to the filtrate and under a nitrogen atmosphere the mixture was refluxed with stirring for 12.5 h. To the hot reaction mixture was added potassium tetrachloroplatinate(II) (0.64 g, 1.54 mmol) dissolved in a small amount of ethane-1,2-diol. Immediately the solution was neutralized with glacial acetic acid as confirmed by pH test paper. After neutralization, reflux was continued for more than 6 h during which dark green precipitates gradually appeared. After reflux, the hot reaction mixture was filtered and the dark green precipitate collected on filter paper. The product was dissolved in chloroform and the solvent evaporated to give dark green liquid crystals. Purification was carried out by column chromatography [silica gel, chloroform–benzene (1 : 1 v/v), $R_f=0.70$] and reprecipitation carried out by adding acetone to a hot solution of the product in chloroform to give dark green liquid crystals (0.37 g, yield: 10%).

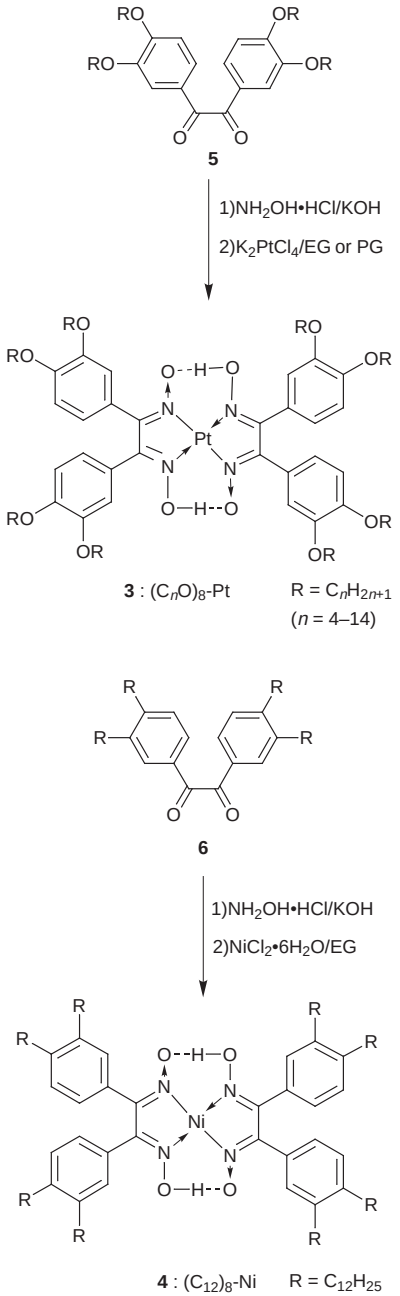

Scheme 1 Synthetic routes to long chain-substituted bis(diphenylglyoximato)metal(II) complexes; EG = ethane-1,2-diol, PG = propane-1,3-diol

2.2 Measurements

The products were characterized by elemental analyses using a Perkin Elmer 240B Elemental Analyzer. The phase transition behavior of the compounds was observed by a polarizing microscope equipped with a heating plate controlled by a thermoregulator (Mettler FP80 and FP82), and heat changes measured with a Rigaku Thermoflex DSC-10A or a Shimadzu DSC-50 differential scanning calorimeter. To establish the mesophases, powder X-ray patterns were measured with Cu-Kα radiation using a Rigaku Geigerflex instrument equipped with a hand-made heating plate controlled by a thermoregulator.[17] Temperature-dependent electronic spectra were recorded with a Hitachi 330 spectrophotometer equipped with a hand-made heating plate controlled by a thermoregulator (CHINO DB-125).[17] For thermochromism measurements, thin films of the Ni and Pt complexes were prepared by casting from a solution of the products in chloroform on glass. Glass Techno, P-102 glass was used, since it is transparent in the wavelength range 250–2100 nm. Measurements were carried out in air as reference.

3 Results and Discussion

3.1 Mesomorphic properties

We have already reported that each of the $(C_nO)_8$-Ni **1** and -Pd **2** complexes (Fig. 1) has a discotic hexagonal disordered columnar mesophase (Col_{hd}), and that the mesomorphic structure has a linear chain of metals which originates the nd_{z^2}–$(n+1)p_z$ transition of the metal ion.[2,4] For the present complexes, $(C_nO)_8$-Pt ($n=4$–14) **3** and $(C_{12})_8$-Ni **4**, these mesophases are identified by DSC measurements, polarizing microscopy observations and temperature-dependent X-ray diffraction measurements.

3.1.1 Mesomorphic properties of the $(C_nO)_8$-Pt ($n=4$–14) complexes, 3. As is shown in Table 2, each of the $(C_nO)_8$-Pt ($n=4$–14) complexes shows an enantiotropic columnar mesophase. The $(C_nO)_8$-Pt complexes for $n\geqslant 7$ are in a viscous liquid crystalline state at r.t., whereas the $(C_4O)_8$-Pt complex is in a supercooled mesomorphic state and the $(C_nO)_8$-Pt ($n=5$, 6) complexes are in a crystalline state at r.t. A fan-shaped natural texture was observed on cooling for each of the $(C_nO)_8$-Pt complexes for $n\geqslant 6$. Generally this texture is characteristic of a Col_{hd} mesophase. X-Ray diffraction of each of the $(C_nO)_8$-Pt complexes for $n=4$–14 gave spacings in the ratios, $1:1/\sqrt{3}:1/2:1/\sqrt{7}:\cdots$, which correspond to a two-dimensional hexagonal lattice, and a diffuse band at $2\theta\approx 25°$ corresponding to fluctuation of the one-dimensional molecular stack. Hence,

Table 1 Reaction solvents, solvents for the metal salt, elemental analysis data, yields, colors and pristine states of the $(C_nO)_8$-Pt (n=4–14) complexes, **3**, and $(C_{12})_8$-Ni complexes, **4**

n	reaction solvent (v/v)	solvent for the metal salt	elemental analysis (%) found (calc.) C	H	N	yield[a] (%)	color	pristine state[b]
4	MeOH–EtOH(1:1)	EG	57.38(57.63)	7.00(6.93)	4.39(4.48)	4	dark green	supercooled Col_{hd}
5	EtOH	EG	59.97(59.94)	7.53(7.55)	4.00(4.11)	21	dark green	K_1
6	EtOH	EG	62.21(61.89)	8.08(8.80)	3.68(3.80)	7	dark green	K
7	EtOH	EG	63.91(63.57)	8.47(8.51)	3.48(3.53)	9	dark green	Col_{hd}
8	MeOH–EtOH(1:1)	EG	65.31(65.03)	9.02(8.90)	3.18(3.30)	8	dark green	Col_{hd}
9	EtOH	EG	66.38(66.30)	9.19(9.24)	3.01(3.09)	8	dark green	Col_{hd}
10	EtOH	EG	67.53(67.43)	9.54(9.54)	2.79(2.91)	8	dark green	Col_{hd}
11	EtOH	EG	68.72(68.43)	9.85(9.80)	2.68(2.72)	4	dark green	Col_{hd}
12	EtOH	PG	69.20(69.33)	10.05(10.04)	2.56(2.61)	8	dark green	Col_{hd}
13	EtOH	EG	70.34(70.14)	10.18(10.26)	2.41(2.48)	9	dark green	Col_{hd}
14	EtOH	EG	70.56(70.87)	10.49(10.45)	2.28(2.36)	10	dark green	Col_{hd}
$(C_{12})_8$-Ni	EtOH	EG	79.05(77.78)	11.45(11.21)	2.97(2.64)	6	red	Col_{rh}

[a]Recrystallization solvent: $CHCl_3$–acetone. [b]K = crystal, Col_{hd} = hexagonal disordered columnar mesophase, Col_{ro} = rectangular ordered columnar mesophase.

Table 2 Phase transition temperatures (T/°C) and enthalpy changes (ΔH/kJ mol^{-1} in parentheses) for the $(C_nO)_8$-Pt (n=4–14) complexes, **3**[a]

n	phase transitions
4	supercooled Col_{hd} ⇝ $K_1 \xrightarrow[(3.07)]{206.9} K_2 \xrightarrow[(4.42)]{272.5} Col_{hd} \xrightarrow{312.5}$ IL (Decomp.)
5	$K_1 \xrightarrow[(1.01)]{219.7} K_2 \xrightarrow[(1.99)]{252.9} Col_{hd} \xrightarrow{303.2}$ IL (Decomp.)
6	$K \underset{}{\overset{224.4}{\rightleftharpoons}} Col_{hd} \overset{285.4}{\rightleftharpoons}$ IL (1.25) (20.0)
7	$Col_{hd} \overset{281.5}{\rightleftharpoons}$ IL (20.1)
8	$Col_{hd} \overset{268.8}{\rightleftharpoons}$ IL (17.8)
9	$Col_{hd} \overset{263.3}{\rightleftharpoons}$ IL (18.2)
10	$Col_{hd} \overset{255.5}{\rightleftharpoons}$ IL (17.7)
11	$Col_{hd} \overset{247.3}{\rightleftharpoons}$ IL (16.2)
12	$Col_{hd} \overset{239.3}{\rightleftharpoons}$ IL (16.4)
13	$Col_{hd} \overset{232.8}{\rightleftharpoons}$ IL (15.9)
14	$Col_{hd} \overset{227.8}{\rightleftharpoons}$ IL (15.6)

[a]K = crystal, Col_{hd} = hexagonal disordered columnar mesophase, IL = isotropic liquid, Decomp. = decomposition, ⇝ = relaxation.

each of these mesophases can be assigned to a Col_{hd} mesophase, as well as those of the $(C_nO)_8$-Ni and Pd complexes. The assignment is also consistent with the fan-shaped texture. Phase transition temperatures of the $(C_nO)_8$-Pt complexes for n=4–14 are plotted *vs.* the carbon number (n) in the alkoxy chain in Fig. 2. This figure clearly shows that the melting point of the Pt complexes becomes lower upon increasing the chain length and the temperature region of the mesophase consequently becomes larger. As Table 3 shows, the clearing points of $(C_{12}O)_8$-M complexes for M = Ni, Pd, Pt are higher in the

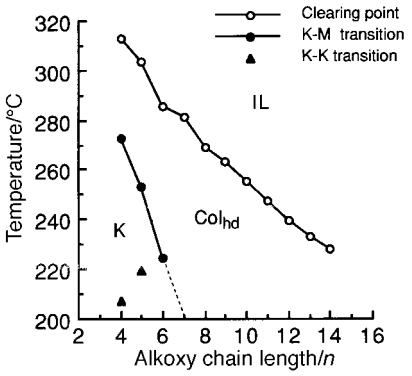

Fig. 2 Phase transition temperatures *vs.* the number of carbon atoms (n) in the alkoxy chains of the $(C_nO)_8$-Pt (n=4–14) complexes, **3**

Table 3 Comparison of phase transition temperatures (°C) enthalpy changes (ΔH/kJ mol^{-1} in parentheses) and X-ray data of the $(C_{12}O)_8$-M (M = Ni, Pd, Pt) and $(C_{12})_8$-Ni complexes **1–4**

complex		phase transitions
$(C_{12}O)_8$-Ni	**1**[a]	$Col_{hd} \overset{211(36.9)}{\rightleftharpoons}$ IL (a = 34.4 Å at r.t.)
$(C_{12}O)_8$-Pd	**2**[b]	$Col_{hd} \overset{229(23.5)}{\rightleftharpoons}$ IL (a = 35.4 Å at r.t.)
$(C_{12}O)_8$-Pt	**3**	$Col_{hd} \overset{239.3(16.4)}{\rightleftharpoons}$ IL (a = 34.2 Å at 150°C)
$(C_{12})_8$-Ni	**4**	$Col_{ro}(P2/a) \overset{32.1(46.6)}{\rightleftharpoons} Col_{hd} \overset{82.3(23.1)}{\rightleftharpoons}$ IL (a = 61.7, b = 46.6, h = 3.37 Å at 22 °C) (a = 33.7 Å at 60 °C)

[a]Ref. 2 and 3. [b]Ref. 4.

order of $(C_{12}O)_8$-Ni < $(C_{12}O)_8$-Pd < $(C_{12}O)_8$-Pt, so that the temperature region of the mesophase also becomes larger in this order.

3.1.2 Effects of long chains on the liquid crystalline $(DPG)_2$Ni derivatives, 1 and 4. We have already reported the influence of long chains on substituted β-diketonato copper complexes[18] and dithiolene nickel complexes.[16,19] Interestingly, these complexes have mesomorphic properties when the chain is an octyloxy group, whereas they do not show mesophases when the chain is an octyl group. Hence, we wished to investigate

the influence of different long-chain-substituents for the core bis(diphenylglyoximato)metal(II) derivatives, $(DPG)_2M$, on their mesomorphic properties. We investigated the Ni derivatives, since the syntheses of the dodecyl-substituted Pd and Pt derivatives were not successful whereas the dodecyl-substituted Ni derivative was obtained (Fig. 1). It has been already reported in a previous paper[17] that $(C_{12}O)_8$-Ni **1**, shows a Col_{hd} mesophase for which the lattice constant a is 34.4 Å at r.t. Table 3 summarizes the phase transition temperatures, enthalpy changes and X-ray data of $(C_{12}O)_8$-Ni **1** and $(C_{12})_8$-Ni **4**.

X-Ray diffraction of the lower temperature mesophase of $(C_{12})_8$-Ni **4**, at 22 °C gave reflections from a two-dimensional rectangular lattice with $a=61.7$ Å and $b=46.6$ Å. Since Z could be estimated to be *ca.* 4 in the unit cell and since the Miller indices $(0k)$ were absent when k was odd, it could be concluded that the rectangular lattice has $P2/a$ symmetry. In addition, a reflection appeared at $2\theta\approx25°$ which corresponds to a one-dimensional stack of the molecules with an interdisk separation h of 3.37 Å. Hence, the lower temperature mesophase could be identified as a rectangular ordered columnar mesophase, Col_{ro} $(P2/a)$. X-Ray diffraction of the higher temperature mesophase at 60 °C gave a diffuse band at $2\theta\approx25°$ corresponding to fluctuation of the molecular stack and reflections from a two-dimensional hexagonal lattice having lattice constant $a=33.7$ Å. Therefore, the higher temperature mesophase in the region from 31.2–82.3 °C could be identified as a Col_{hd} mesophase, as for $(C_{12}O)_8$-Ni. A fan-shaped texture was observed. A schematic representation of the mesomorphic structural change from the Col_{ro} mesophase to the Col_{hd} mesophase is shown in Fig. 3. The molecular planes tilt to the rectangular plane in the lower temperature mesophase. On the other hand, the molecules begin to rotate by thermal movement in the higher temperature mesophase region, so that they are packed in a hexagonal lattice. As can be seen in Fig. 3, the two-dimensional lattice expands to $67.4/61.7=1.09$ times in the a-axis direction and $58.4/46.6=1.25$ times in the b-axis direction.

3.2 'Visible fastener effect' on mesomorphic thermochromism

3.2.1 'Apparent pressure' by surrounding long chians. We have already reported that the alkoxy-chain-substituted bis(diphenylglyoximato)nickel(II)[2,3] and palladium(II)[4] complexes, $(C_nO)_8$-Ni **1** and $(C_nO)_8$-Pd **2** (Fig. 1), exhibit color changes with increasing temperature. The Ni and Pd complexes gradually turn from red to yellow and from orange to yellow, respectively. On the other hand, the present alkoxy chain-substituted bis(diphenylglyoximato)platinum(II) complexes, $(C_nO)_8$-Pt **3**, synthesized here exhibit sharp color changes from green at r.t. to red, orange, and yellow with increasing temperature, as is shown in Fig. 4 and 5. The natural texture of the

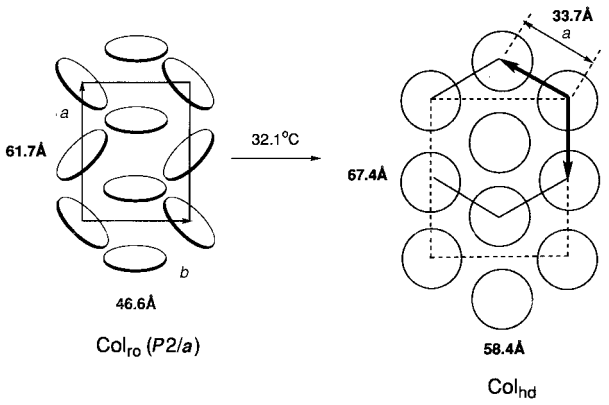

Fig. 3 Schematic representation of the mesomorphic structural change from Col_{ro} to Col_{hd} for the $(C_{12})_8$-Ni complex, **4**

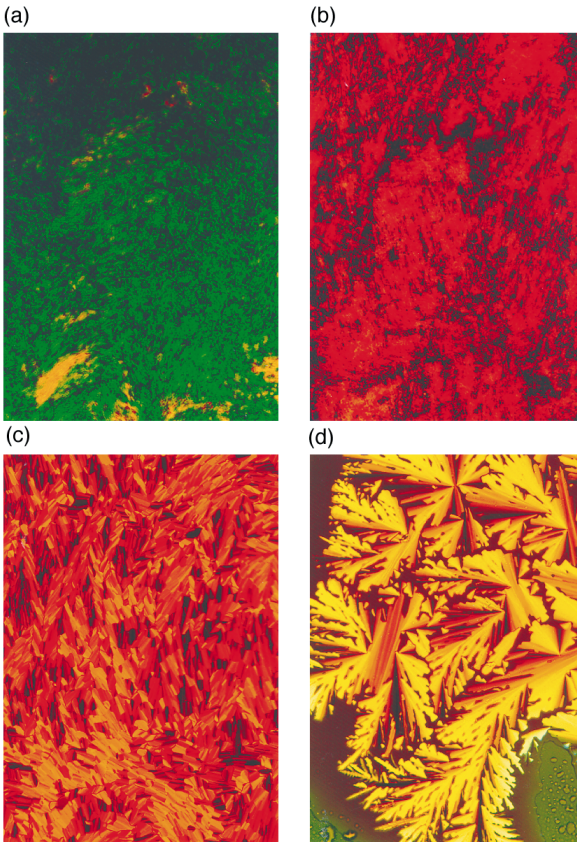

Fig. 4 Photomicrographs of the $(C_{12}O)_8$-Pt complex at various temperatures: (a) r.t., (b) 200 °C, (c) 235 °C and (d) 238 °C

discotic mesophase was observed as yellow and fan like when the yellow isotropic liquid(IL) at >239.3 °C was cooled to 238 °C [Fig. 4(d)]. Shirotani *et al.*[8] reported that the $5d_{z^2}$–$6p_z$ transition band of Pt^{2+} which is consistent with a one-dimensional platinum stack is located at 18 200 cm^{-1} at atmospheric pressure, and that the band shifts toward lower energy by -3000 cm^{-1} GPa^{-1}. By using this shift coefficient the 'apparent pressure' on the present long-chain-substituted Pt complex could be estimated from eqn. (1)

$$\text{Pressure GPa}=\frac{(\tilde{\nu}_{obs}-18\,200)\ \text{cm}^{-1}}{-3000\ \text{cm}^{-1}\ \text{GPa}^{-1}} \qquad (1)$$

where $\tilde{\nu}_{obs}$ is the observed wavenumber of the d–p band. The d–p band of the $(C_{12}O)_8$-Pt complex is located at 15 600cm^{-1} (641 nm) at 35 °C so the 'apparent pressure' can be estimated to be 0.87 GPa at atmospheric pressure.

3.2.2 Influences of metals on the 'fastener effect'. Fig. 5(a)–(c) show electronic spectra at various temperatures for the $(C_{12}O)_8$-Ni, Pd and Pt complexes, respectively. Comparison with the detailed assignment of electronic spectra for the $(C_{12}O)_8$-Pd complex in a previous paper,[4] the A and B bands can be assigned to the nd_{z^2}–$(n+1)p_z$ transition of M^{2+} and to a metal to ligand charge transfer transition (MLCT), respectively; band C has not been assigned.[4] As can be seen from this figure, the A band of the $(C_{12}O)_8$-Pt complex at 641 nm at 35 °C shifts to higher energy (blue-shift) with increasing temperature more than the A bands of the Ni and Pd complexes (located at 550 and 467 nm at 35 °C, respectively). This blue-shift can be reasonably explained by an increase of the intermolecular distance within the columns. The d–p band wavenumbers of each of the metal complexes are plotted *vs.* temperature in Fig. 6(a). A linear relationship between the d–p band wavenumber and temperature is observed. Table 4 lists the rates of blue-shift as determined by least-squares. It is clear that the

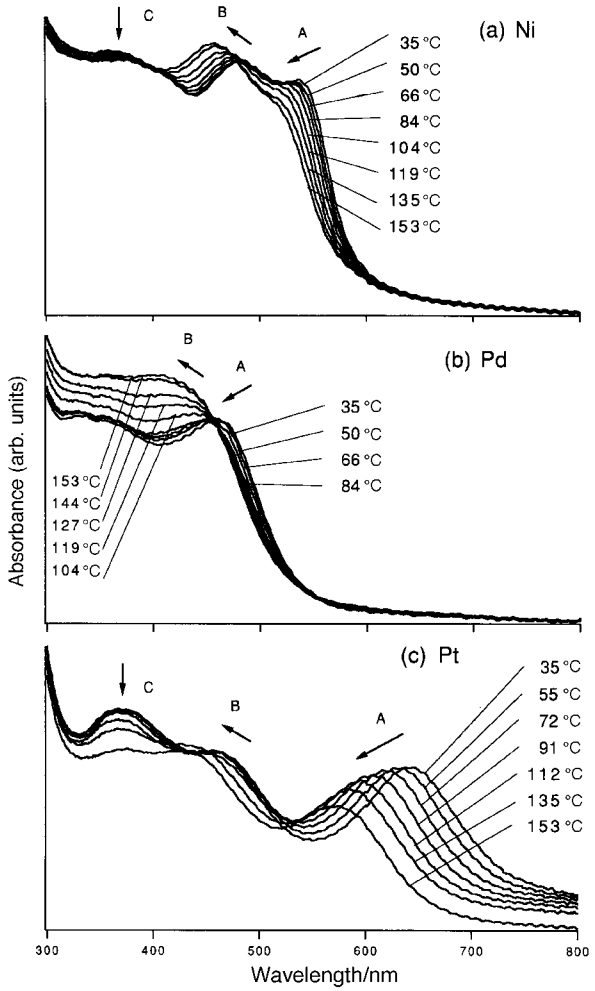

Fig. 5 Electronic absorption spectra of a thin film of the $(C_{12}O)_8$-M complexes at various temperatures: (a) M = Ni, (b) Pd, and (c) Pt. According to the assignment in the literature,[19] A band = nd_{z^2}–$(n+1)p_z$ transition(B_{1u}) and B band = metal-to-ligand charge transfer transition (MLCT: B_{2u} or B_{3u}). The C band has not been reported previously.

Pt complex exhibits the largest blue-shift-rate, the rates being in the order $(C_{12}O)_8$-Ni < $(C_{12}O)_8$-Pd < $(C_{12}O)_8$-Pt. By using these shift-rates and the wavenumber of the d–p bands at various temperature, 'apparent pressures' were calculated from eqn. (2) in the same manner as for eqn. (1)

$$\text{Pressure GPa} = \frac{\tilde{\nu}_{\text{obs}} - X}{Y} \qquad (2)$$

where X cm^{-1} and Ycm^{-1} GPa^{-1} are the wavenumber of the d–p transition band under atmospheric pressure and the blue-shift-rate of the non-substituted core $(DPG)_2M$ complex, respectively. X and Y values and the 'apparent pressures' of $(C_{12}O)_8$-Ni, Pd and Pt complexes at 35 °C are summarized in Table 5. As can be seen from Fig. 6(b), all complexes have a similar linear relationship between temperature and apparent pressure with slopes of *ca.* -5×10^{-3} GPa °C^{-1}. This means that the 'apparent pressure' on the central core complex imparted by the fastener effect of the surrounding long chains is released by *ca.* -5×10^{-3} GPa °C^{-1} with increasing temperature, irrespective of the central metal.

Thus, under atmospheric pressure long-chain-substituted bis(diphenylglyoximato)metal(II) complexes are self-pressed by van der Waals interaction between the surrounding long chains, as if they were subject to an external high pressure. With increasing temperature the apparent pressure is gradually weakened and the interdisk distance within the column extends until finally the columnar structure disintegrates into discrete

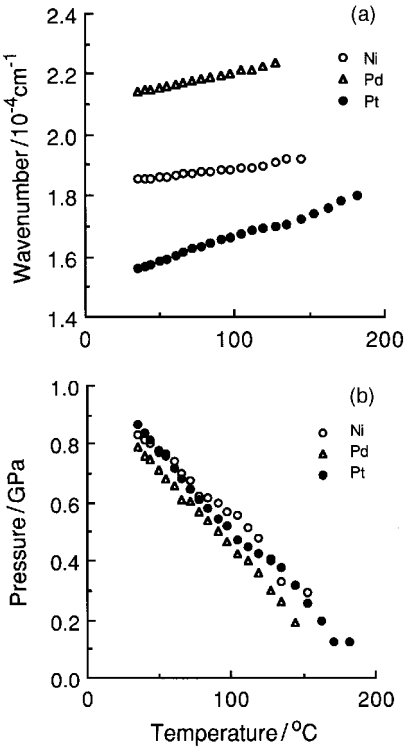

Fig. 6 (a) Wavenumbers of the d–p bands and (b) apparent pressures at various temperatures for the $(C_{12}O)_8$-M (M = Ni, Pd, Pt) complexes

Table 4 Rates of blue-shift of the d–p bands for the $(C_{12}O)_8$-M (M = Ni, Pd, Pt) complexes with increasing temperature

M	rate of blue-shift (cm^{-1} °C^{-1})
Ni	6.07
Pd	10.1
Pt	15.6

Table 5 Shifts of pressure and values of apparent pressure at 35 °C for the $(C_{12}O)_8$-M (M = Ni, Pd, Pt) complexes

M	X^a/ cm^{-1}	Y^a/cm^{-1} GPa^{-1}	pressure/GPa at 35 °C
Ni	19610	−1300	0.83
Pd	22940	−1940	0.79
Pt	18200	−3000	0.87

[a]Ref. 8.

molecules at the clearing point. The expansion of the interdisk distance with increasing temperature corresponds to an expansion of metal–metal distance in the one-dimensional metal chain which is the origin of the blue-shift of the d–p band leading to thermochromism. Thus, measurements of the temperature-dependent electronic spectra enable us to reasonably elucidate the relationship between the 'fastener effect' and the mechanism of thermochromism.

The different rates of blue-shift (Table 4) can be explained by the different size of the metal ions. Shirotani *et al.*[8] reported the rates of red-shift of the d–p bands *vs.* pressure for bis(1,2-cyclohexanedione dioximato)metal(II) complexes $[(NIOX)_2M]$, bis(dimethylglyoximato)metal(II) complexes $[(DMG)_2M]$ and bis(diphenylglyoximato)metal(II) complexes $[(DPG)_2M]$; the rates of red-shift increase in the order $(NIOX)_2M < (DMG)_2M < (DPG)_2M$ for a given central metal. This means that the $(DPG)_2M$ complex having the bulkiest ligand shows the largest rate of red-shift; on the other hand, rates are in the order of Ni < Pd < Pt complex for a given ligand. Drickamer *et al.* also reported a similar order for the

metals.[20,21] Since the radii are in the order of $Ni^{2+} > Pd^{2+} > Pt^{2+}$, platinum has the smallest ion radius among these metals. When the complex has both the bulkiest ligand (DPG) and the smallest metal ion (Pt^{2+}), it has the loosest metal–metal distance in the one-dimensional metal chain to originate the biggest rate of red-shift of the d–p band with pressure.[8] The present Col_{hd} mesophases of the long chain- substituted $(C_{12}O)_8$-M complexes have a columnar structure containing one-dimensional metal–metal stacks. The $(C_{12}O)_8$-Pt complex has the loosest metal–metal stack among the $(C_{12}O)_8$-M complexes (M = Ni, Pd, Pt). Such a structure leads to the largest blue-shift of the d–p band with temperature, leading to the most drastic 'mesomorphic thermochromism'.

Hence, it can be concluded that the compressibility of the one-dimensional metal–metal stacking distance and the resulting delocalization of d-electrons depends on the bulkiness of the ligands and the size of the metal ions, and that they can be sensitively varied by the apparent pressure of the fastener effect of the surrounding long chains.

3.2.3 Influence of the length of long chains on fastener effect. As mentioned above, the nature of the metal crucially influences the thermochromism of the alkoxy-chain-substituted complexes, $(C_nO)_8$-M **1**–**3**. Fig. 7 shows the variation of the wavenumber of the d–p bands and the 'apparent pressures' at r.t. plotted *vs.* the number (n) of carbon atoms in the alkoxy chains of the $(C_nO)_8$-Pt complexes, respectively. As can be seen in Fig. 7, the d–p band shows a discontinuity between $n = 5$ and 6; the reason for this behaviour is not clear at the present time. As can also be seen in Fig. 7, it seems that 'apparent pressure' *via* the 'fastener effect' attains a plateau at *ca.* 0.9 GPa at $n \geqslant 12$. In other words, the 'fastener effect' may not work effectively for highly extended alkoxy chains.

3.2.4 Influence of the nature of long chains on the fastener effect. We next investigated the influence of the nature of the surrounding long chains on the 'fastener effect' and thermochromism; the dodecyloxy chains were replaced by dodecyl-chains to give the $(C_{12})_8$-Ni complexes.

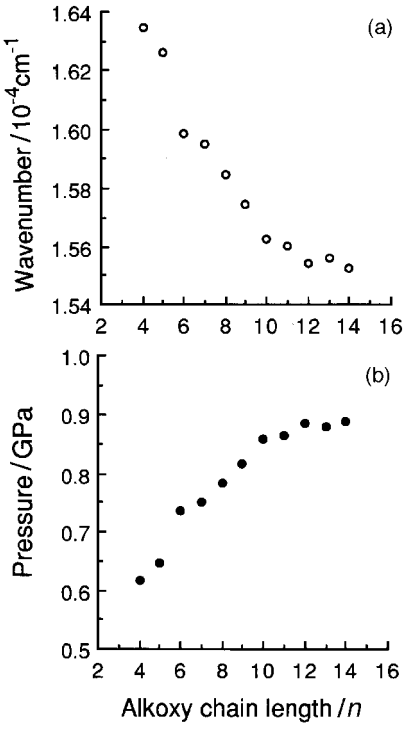

Fig. 7 (a) Wavenumbers of the d–p bands and (b) apparent pressures *vs.* the number of carbon atoms (n) in the alkoxy chains of the $(C_nO)_8$-Pt ($n = 4$–14) complexes, **3**, at r.t.

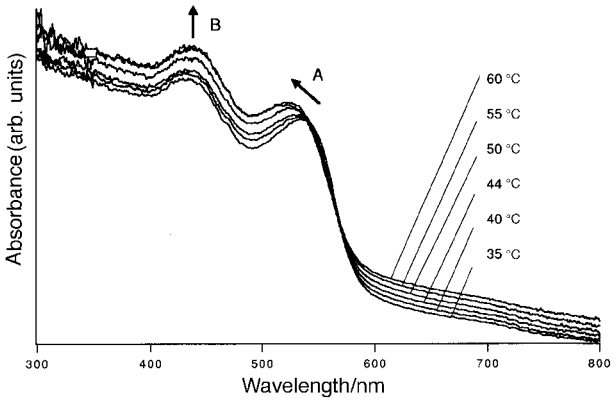

Fig. 8 Electronic absorption spectra of a thin film of the $(C_{12})_8$-Ni complex at various temperatures: (a) M = Ni, (b) Pd, and (c) Pt. According to the assignment in the literature,[19] A band = nd_{z^2}–$(n+1)p_z$ transition (B_{1u}) and B band = metal-to-ligand charge transfer transition (MLCT : B_{2u} or B_{3u}).

Fig. 8 shows electronic spectra of a thin film of the $(C_{12})_8$-Ni complex at various temperatures. The A and B bands of this $(C_{12})_8$-Ni complex show different behavior from those of the $(C_{12}O)_8$-M complexes for M = Ni, Pd and Pt, (Fig. 5). The A band of the $(C_{12})_8$-Ni complex shows a blue-shift with increasing temperature, as does the $(C_{12}O)_8$-Ni complex, however its intensity increases with increasing temperature in direct contrast to the $(C_{12}O)_8$-Ni complex. The intensity of the B band of the $(C_{12})_8$-Ni complex increases with increasing temperature, similarly to the $(C_{12}O)_8$-Ni complex, but shows no blue-shift in contrast to the $(C_{12}O)_8$-Ni complex. Irrespective of these different behaviors, the A and B bands of the $(C_{12})_8$-Ni complex can be assigned to the $3d_{z^2}$–$4p_z$ transition Ni^{2+} and the metal–ligand charge transfer (MLCT) band, respect-

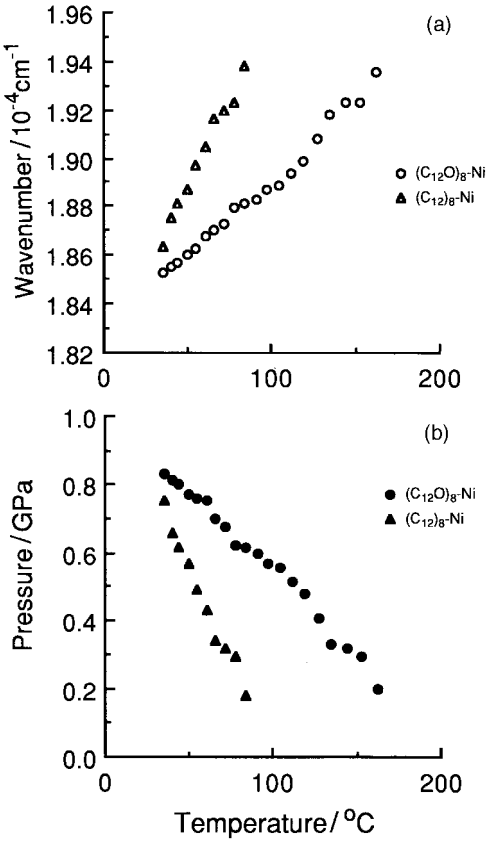

Fig. 9 (a) Wavenumbers of the d–p bands and (b) apparent pressures at various temperares for Col_{hd} mesophases of the $(C_{12}O)_8$-Ni and $(C_{12})_8$-Ni ($n = 4$–14) complexes, **1** and **4** (temperature $\geqslant 35$ °C)

ively, since their band positions are approximately the same as those of the $(C_{12}O)_8$-Ni complex. These assignments are also supported by the disappearance of the A band in a solution of the $(C_{12})_8$-Ni complex in chloroform, similarly to the $(C_{12}O)_8$-Ni complex.[2,3] Fig. 9 shows the d–p bands and the 'apparent pressures' at r.t. *vs.* temperatures, respectively, for the $(C_{12}O)_8$-Ni and $(C_{12})_8$-Ni complexes. The 'apparent pressure' decreases with increasing temperature at a rate of *ca.* -1.1×10^{-2} GPa °C^{-1} for the $(C_{12})_8$-Ni complex. This rate is about twice that of $(C_{12}O)_8$-Ni (*ca.* -5×10^{-3} GPa °C^{-1}). The difference of the rates between these complexes may be due to the presence of oxygen atoms, since the dodecyloxy group is more electron-donating than the dodecyl group, the core complex part of the $(C_{12}O)_8$-Ni complex becomes very electron rich so that the intermolecular interactions of the core $(C_{12}O)_8$-Ni complex are stronger than that of $(C_{12})_8$-Ni. Hence, the $(C_{12}O)_8$-Ni molecules more strongly adhere with each other at the core complex part than do $(C_{12})_8$-Ni molecules. When they are heated, the 'apparent pressure' of the surrounding long chains is reduced so that their core complex parts should be released from the 'fastener effect'. However, the strong interaction between the core complex parts of the $(C_{12}O)_8$-Ni complex may persist at higher temperatures compared with the $(C_{12})_8$-Ni complex.

4 Conclusion

We have described the influence of central metals and the surrounding long chains on thermochromism of long-chain-substituted bis(diphenylglyoximato)metal(II) complexes. Novel complexes $(C_nO)_8$-Pt ($n=4$–14) and $(C_{12})_8$-Ni were prepared. It was revealed that the long-chain-substituted bis(diphenylglyoximato)metal(II) complexes exhibit not only mesomorphic properties but also thermochromism caused by the 'fastener effect' of the van der Waals interaction of the peripheral long chains. The length and nature of the long chains influence not only on the mesomorphic properties but also the thermochromism. The one-dimensional metal stacking structure is central to this thermochromism. The value of 'apparent pressure' was estimated to be 0.87 GPa for the $(C_{12}O)_8$-Pt complex at 35 °C. The apparent pressure by the surrounding long chains reaches a saturated plateau around 0.9 GPa for $n\geqslant12$ for the $(C_nO)_8$-Pt complexes. The $(C_{12}O)_8$-Pt complex which has the bulkiest ligand and the smallest metal ion exhibits the most drastic thermochromism among the $(C_{12}O)_8$-M complexes for M = Ni, Pd, Pt. Such a visible fastener effect so far as we know is unprecedented. The present thermochromism enables to see van der Waals interactions visually. This work may also represent a new frontier in applications of liquid crystalline organic metal complexes (metallomesogens). In addition, we can expect to obtain high electronic conductivities by such a fastener effect under atmospheric pressure even for the compounds exhibiting high conductivities only under high pressure.

References

1 K. Ohta, S. Azumane, T. Watanabe, S. Tsukada and I. Yamamoto, *Appl. Organomet. Chem*., 1996, **10**, 623.
2 K. Ohta, H. Hasebe, M. Moriya, T. Fujimoto and I. Yamamoto, *Mol. Cryst. Liq. Cryst*., 1991, **208**, 43.
3 K. Ohta, H. Hasebe, M. Moriya, T. Fujimoto and I. Yamamoto, *J. Mater. Chem*., 1991, **1**, 831.
4 K. Ohta, M. Moriya, M. Ikejima, H. Hasebe, T. Fujimoto and I. Yamamoto, *Bull. Chem. Soc. Jpn*., 1993, **66**, 3553, 3559.
5 I. Shirotani, K. Suzuki, T. Suzuki, T. Yagi and M. Tanaka, *Bull. Chem. Soc. Jpn*., 1992, **65**, 1078.
6 I. Shirotani, *Petrotech*, 1993, **16**, 781.
7 I. Shirotani, *Gendai Kagaku*, 1987, **42**, frontispiece, 30.
8 I. Shirotani, Y. Inagaki, W. Utsumi and T. Yagi, *J. Mater. Chem*., 1991, **1**, 1041.
9 I. Shirotani, K. Suzuki and T. Yagi, *Proc. Jpn. Acad., Ser. B*, 1992, **68**, 57.
10 H. Inokuchi, G. Saito, P. Wu, K. Seki, T. B. Tang, T. Mori, K. Imaeda, T. Enoki, Y. Higuchi, K. Inaka and N. Yasuoka, *Chem. Lett*., **1986**,1263.
11 H. Inokuchi, K. Imaeda, T. Enoki, T. Mori, Y. Maruyama, G. Saito, N. Okada, H. Yamochi, K. Seki, Y. Higuchi and N. Yasuoka, *Nature* (*London*), 1987, **329**, 39.
12 Z. Shi, T. Enoki, K. Imaeda, K. Seki, P. Wu, H. Inokuchi and G. Saito, *J. Phys. Chem*., 1988, **92**, 5044.
13 P. Wang, T. Enoki, K. Imaeda, N. Iwasawa, H. Yamochi, H. Urayama, G. Saito and H. Inokuchi, *J. Phys. Chem*., 1989, **93**, 5947.
14 K. Imaeda, T. Mitani, C. Nakano, H. Inokuchi and G. Saito, *Chem. Phys. Lett*., 1990, **173**, 298.
15 J. K. Jeszuka, T. Enoki, Z. Shi, K. Imaeda, H. Inokuchi, N. Iwasawa, H. Yamochi and G. Saito, *Mol. Cryst. Liq. Cryst*., 1991, **196**, 167.
16 K. Ohta, H. Hasebe, H. Ema, M. Moriya, T. Fujimoto and I. Yamanoto, *Mol. Cryst. Liq. Cryst*., 1991, **208**, 21.
17 H. Ema, Master Thesis, Shinshu University, Ueda, 1988, ch. 7; H. Hasebe, Master Thesis, Shinshu University, Ueda, 1991, ch. 5.
18 K. Ohta, H. Ema, H. Muroki, I. Yamamoto and K. Matsuzaki, *Mol. Cryst. Liq. Cryst*., 1987, **147**, 61.
19 K. Ohta, H. Hasebe, M. Moriya, T. Fujimoto and I. Yamamoto, *Mol. Cryst. Liq. Cryst*., 1991, **208**, 33.
20 J. C. Zahner and H. G. Drickamer, *J. Chem. Phys*., 1960, **33**, 1625.
21 M. Tkacz and H. G. Drickamer, *J. Chem. Phys.,* 1986, **85**, 1184.

Paper 8/00894IK; *Received* 2nd *February*, 1998